 ICES-2015-265

Design Evolution of the Wide Field Infrared Survey Telescope using Astrophysics Focused Telescope Assets (WFIRST-AFTA) and Lessons Learned

Hume L. Peabody[1], Carlton V. Peters[2], Juan E. Rodriguez-Ruiz[3], Carson S. McDonald[4], David A.Content[5], and Clifton E. Jackson[6]
NASA Goddard Space Flight Center, Greenbelt MD 20771

The design of the Wide Field Infrared Survey Telescope using Astrophysics Focused Telescope Assets (WFIRST-AFTA) continues to evolve as each design cycle is analyzed. In 2012, two Hubble sized (2.4 m diameter) telescopes were donated to NASA from elsewhere in the Federal Government. NASA began investigating potential uses for these telescopes and identified WFIRST as a mission to benefit from these assets. With an updated, deeper, and sharper field of view than previous design iterations with a smaller telescope, the optical designs of the WFIRST instruments were updated and the mechanical and thermal designs evolved around the new optical layout. Beginning with Design Cycle 3, significant analysis efforts yielded a design and model that could be evaluated for Structural-Thermal-Optical-Performance (STOP) purposes for the Wide Field Imager (WFI) and provided the basis for evaluating the high level observatory requirements. Development of the Cycle 3 thermal model provided some valuable analysis lessons learned and established best practices for future design cycles. However, the Cycle 3 design did include some major liens and evolving requirements which were addressed in the Cycle 4 Design. Some of the design changes are driven by requirements changes, while others are optimizations or solutions to liens from previous cycles. Again in Cycle 4, STOP analysis was performed and further insights into the overall design were gained leading to the Cycle 5 design effort currently underway. This paper seeks to capture the thermal design evolution, with focus on major design drivers, key decisions and their rationale, and lessons learned as the design evolved.

Nomenclature

AFTA	=	Astrophysics Focused Telescope Assets
AMS	=	Aft Metering Structure
CAD	=	Computer Aided Design
CGI	=	Coronagraph Instrument
FPA	=	Focal Plane Assembly
GSFC	=	Goddard Space Flight Center
IFU	=	Integral Field Unit
JPL	=	Jet Propulsion Laboratory
NASA	=	National Aeronautics and Space Administration
OB	=	Optical Bench
PID	=	Proportional-Integral-Derivative control
STOP	=	Structural-Thermal-Optical-Performance
WFI	=	Wide Field Instrument
WFIRST	=	Wide Field Infra-Red Survey Telescope

[1] Staff Thermal Engineer, Mail Stop 545, Goddard Space Flight Center, Greenbelt MD 20771
[2] Thermal Engineering Associate Branch Head, Mail Stop 545, Goddard Space Flight Center, Greenbelt MD 20771
[3] Thermal Engineer, Mail Stop 545, Goddard Space Flight Center, Greenbelt MD 20771
[4] Thermal Engineer, Edge Space Systems, P.O. Box 310 Glenelg MD 21737
[5] Payload Systems Manager, Mail Stop 448, Goddard Space Flight Center, Greenbelt MD 20771
[6] Instrument Systems Engineer, SGT, Inc., 7701 Greenbelt Road, Suite 400, Greenbelt MD 20771

I. INTRODUCTION

THE Wide Field InfraRed Survey Telescope (WFIRST) mission was selected as the top-ranked large space mission in the 2010 New Worlds, New Horizons Astronomy and Astrophysics Decadal survey. WFIRST utilizes the Astrophysics Focused Telescope Assets (AFTA) donated from elsewhere in the Federal Government to study Dark Energy, Exoplanets, and the near infrared sky. AFTA consists of an existing 2.4 m diameter telescope and provides the front end optics to direct incoming energy to a pair of instruments supported by an Instrument Carrier. The first of these two instruments, the Wide Field Instrument (WFI) utilizes a 3x6 array of H4RG detectors to provide a sky field of view nearly 100x larger than the Wide Field Camera 3 instrument on the Hubble Space Telescope. Furthermore, the WFI includes a secondary Integral Field Unit (IFU) channel which uses a slicer and spectrograph to provide individual spectra of each slice. The WFI provides wide field imaging and slitless spectroscopic capabilities to measure Dark Energy, Exoplanet Microlensing, and the near infra-red sky survey. The second instrument, the CoronaGraph Instrument (CGI), has both an imaging and spectroscopic mode to directly image exoplanets and debris discs around nearby stars.

Being in pre-Phase A, the mission itself has a very wide trade and design space to investigate prior to entering formulation. The overall observatory has undergone significant design evolution over the last few years as requirements have changed or liens against a current design incarnation were identified. Since 2013, three design cycles have been completed, analyzed, and built upon for the next design cycle. During this process, numerous lessons were learned, and this paper seeks to capture each of those designs from a thermal perspective and identify lessons learned as the design matured.

II. WFIRST OVERALL DESIGN

The WFIRST observatory (Figure 1) orbits in a geosynchronous orbit with a sunshield/solar array to provide a stable thermal environment. A modular, serviceable, hexagonal spacecraft bus supports the payload and provides all the attitude control, communications, and other functions necessary for the mission. Three sets of bipods support the aft metering structure (AMS), to which the telescope mounts. Surrounding the telescope is the outer barrel assembly supported by its own set of bipods, which minimizes stray light to the telescope and provides a temperature controlled barrier around the telescope optics. The AMS also supports the Instrument Carrier, which provides the mechanical support and metering structure for the two instruments, WFI and CGI. The instruments are held in place with latches and are designed to be serviced (i.e. replaced) on orbit as are the six spacecraft avionics modules. The instrument warm electronics boxes are also located in the spacecraft modules. However, the specific degree of serviceability has yet to be determined at a mission level.

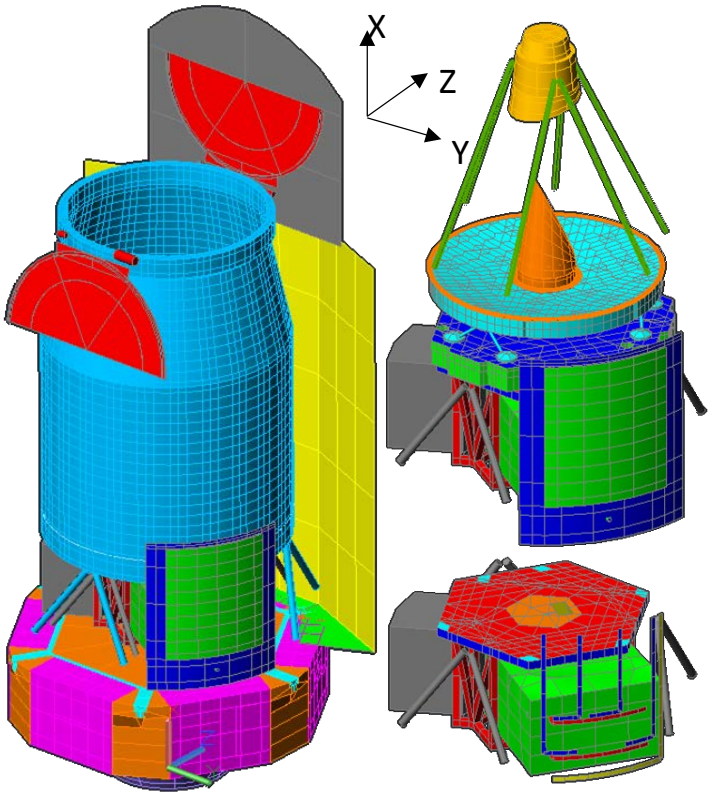

Figure 1. WFIRST Observatory Cycle 3 Thermal Model: *Full observatory (Left), Telescope, AMS, Instrument Carrier, WFI, and CGI (Top Right), and Instrument Carrier, CGI and WFI Enclosure and Heatpipes (Bottom Right).*

The WFIRST mission is a joint mission between NASA-GSFC and JPL. ITT/Exelis built and maintains the existing telescope hardware, which is managed by JPL. JPL also is currently responsible for the definition of the CGI instrument. GSFC is currently the overall mission manager and is responsible for the definition of the spacecraft bus, the WFI instrument and the overall observatory, including integration and test.

III. CYCLE 3 DESIGN

WFIRST Cycle 1 and Cycle 2 designs evolved from using the donated telescope prescription as-is and included only the WFI instrument to a revised telescope prescription and the inclusion of the CGI instrument. The Cycle 3 design was the first WFIRST design to feature the AFTA telescope, include the baseline instrument complement, and have sufficient staffing and funding to reach a level of model maturity to perform Structural-Thermal-Optical-Performance (STOP) analysis. The Cycle 3 Instrument Carrier consists of a top panel sandwich construction with a lower truss structure. The truss structure includes two latches for WFI closest to the AMS and one further away in the -X direction from the AMS. The design for WFI (Figure 2) features a two temperature zone, passive thermal system to maintain temperature and stability for the optical bench (OB) and Focal Plane Assembly (FPA). Incoming light from the telescope is reflected off a flat fold mirror (F1), then a powered mirror (M3), passes through either one of six filters or a grism (grating-prism) located in various positions of an element wheel, and finally reflects off a final, flight-adjustable flat fold mirror (F2) before reaching the FPA. The FPA itself is a 3x6 array of H4RG detectors mounted to a Silicon-Carbide plate that is coupled via methane heat pipes to a large interior radiator with trim heaters to maintain the temperature at 120 K. The central 120 K radiator includes a number of additional methane spreader heatpipes to improve efficiency. The optical bench features embedded ethane heat pipes, which are coupled to an outer picture frame radiator and maintain the OB at 170 K. The bottom pipe couples directly to the 170 K radiator, while the top pipe is coupled via a field joint to an additional pipe connected to the radiator. Lastly, the FPA cold electronics are also coupled to the same 170 K radiator via ethane heat pipes.

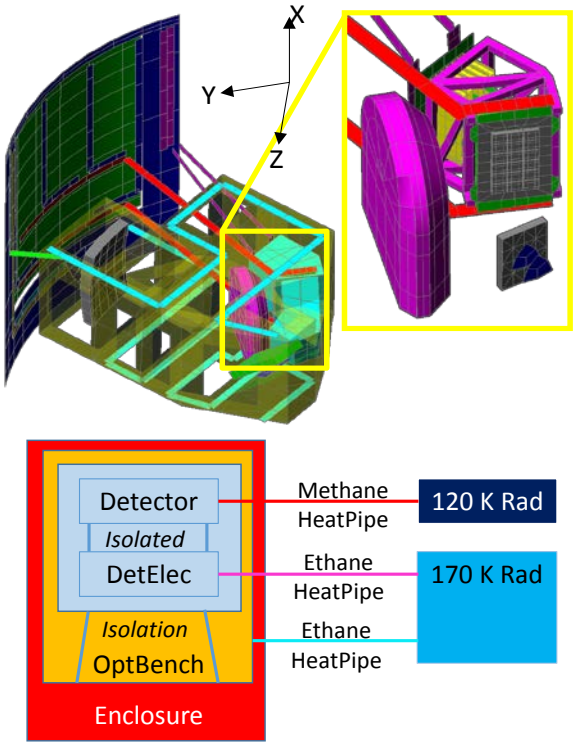

Figure 2. WFI Instrument Cycle 3 Thermal Model: *The optical bench includes two planar ethane heatpipes (cyan) to isothermalize, which are connected to a 170 K picture frame radiator. Two methane heatpipes (red) connect the FPA to a central 120 K radiator. Two ethane heatpipes (magenta) connect the FPA cold electronics to the 170 K radiator. A low conductivity composite frame separates the FPA from the cold electronics.*

IV. CYCLE 3 LESSONS LEARNED

Temperature stability of the FPA and the OB are both important to the WFI instrument. The FPA should be stable to ±0.01 K over a 180 second interval and to ±0.1 K over timescales larger than 180 seconds; the OB should be stable to ±0.5 K over all time scales. For the thermal engineer, this implies the question of what control band and algorithm should be used. If the control were thermostatic in nature (i.e. on/off controller), the band would need to be very tight, with on/off points well within the range over which control should be established. However, for proportional control, this is not true and a very small control band can lead to instability and oscillations in the controller. For proportionally controlled heaters, the on/off setpoints should be larger than the range over which control is desired. Proportional control can address the stability requirements, but if maintaining an absolute temperature is also needed, then a further integral term should be included in the control scheme to account for the drift offset between the achieved temperature and the setpoint. This PI (Proportional-Integral) controller requires a different analytical approach than the simple proportional control option for a heater in the ThermalDesktop software used by the project. Fortunately, the software does include a Generic PID (Proportional-Integral-Derivative) object. However, determining the appropriate gain values for a PID controller is not necessarily something that is typically performed by the thermal engineer.

For classical PID control, the process variable (heater power in this case) is based on three gains and the error, which is defined as the difference between the setpoint and the control variable (in this case sensing temperature). The process variable is computed based on the sum of the proportional gain times the error, the integral gain times

the sum of the error times the timesteps, and the derivative gain times the derivative of the error over the timestep as shown in Equation 1.

$$CV = P_{GAIN} * (SP - PV) + I_{GAIN} * \Sigma (SP - PV)*dt + D_{GAIN} * d(SP - PV)/dt$$

Where: CV = Control Variable (Heater Power)
SP = Setpoint (Temperature to be achieved)
PV = Process Variable (Sensed Temperature)
P_{GAIN}, I_{GAIN}, D_{GAIN} = Proportional, Integral, and Derivative Gain Values
dt = Time Interval

Each of these gains helps to minimize the error. The proportional gain tends to establish the order of magnitude necessary for the process variable to maintain the control variable close to the setpoint. The integral gain helps to minimize the long term drift when the proportional gain alone cannot achieve the desired setpoint. Lastly, the derivative gain helps to maintain control when rapid external effects result in a disturbance of the process variable by applying control based on the rate of change of the error. The impacts of independently varying the different gains can be found in Figure 4, which shows the impact of gain variations on cryocooler performance for the Cycle 4 design discussed in the next section; the baseline performance is shown as the heavy yellow line on each plot. Increasing the proportional gain too far results in oscillating behavior and loss of control, while setting it too low results in significant undershoot of the setpoint. For the case of a proportional heater in ThermalDesktop, the gain is computed from Heater Power / (Off Temp – On Temp). Therefore, setting a very small range would increase the proportional gain and could lead to the instability seen in Figure 3. Increasing the integral gain results in minimizing the long term drift, while lowering it increases the long term drift. Lastly, the increasing the derivative gain results in damping out the oscillations faster, while decreasing it dampens the oscillations out slower. Applying four times the base integral and derivative gains results in much better performance overall.

Understanding these gains and their impact proved valuable to the project. For the long duration thermal model runs, the timesteps to advance the solution are a direct contributor to overall run time. Increasing the solution timestep from 30 s to 60 s resulted in instability of the PID heater controller and oscillating results. Decreasing the proportional gain eliminated the instability and allowed the run time to be reduced with the larger solution timesteps. It should be noted that the gain values may not be in line with the actual gain values of the designed hardware due to the timescales. However, the use of much smaller timescales that the controller acts over would be impractical for use in an observatory level thermal model.

Lesson Learned: For tight temperature control, the inclination to set a small control band may lead to poor performance of a proportional controller. A larger temperature control band will likely improve the stability.

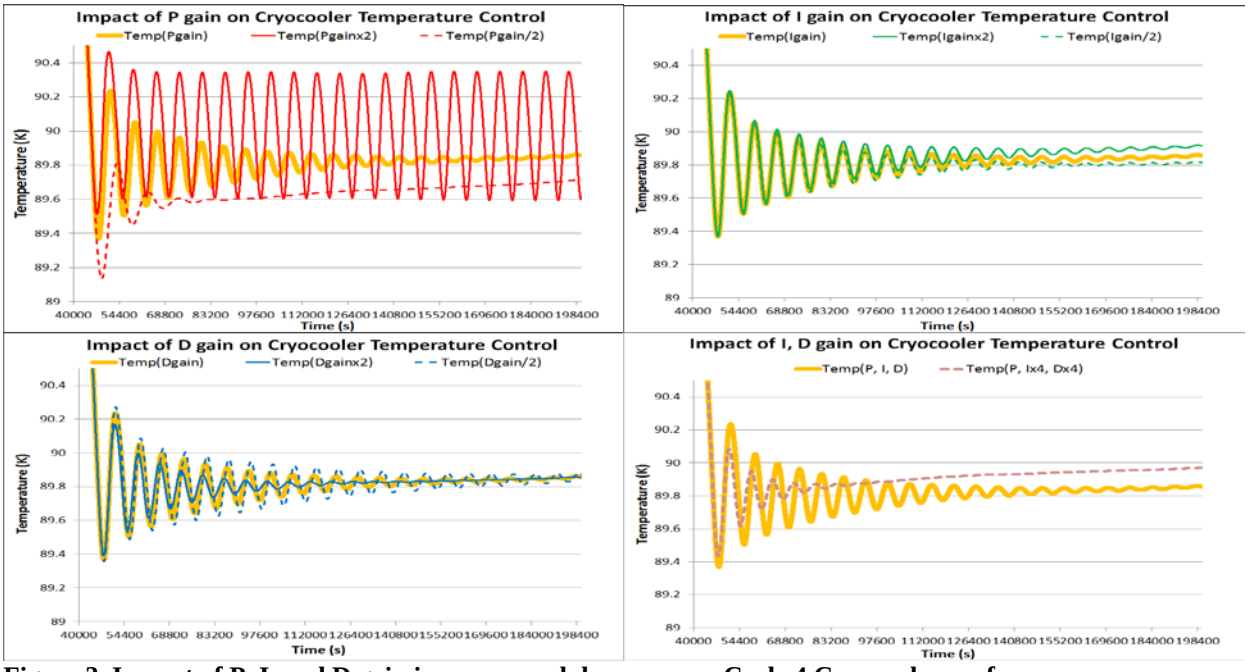

Figure 3. Impact of P, I, and D gain increases and decreases on Cycle 4 Cryocooler performance

Another challenge the team faced was the evaluation of a new software package (during the design process) which specialized in the STOP process. The potential benefit of this software was the generation of both the thermal and structural models from the exact same CAD geometry through the implementation of meshing rules. This eliminates discrepancies between how different thermal and structural analysts may model the same component and what aspects of the CAD model are ignored and provides greater confidence in mapping of thermal results to the structural model. It furthermore includes the ability to define the entire STOP process within the software including the data products passed from model to model and utilizes many industry standard computational codes, including those in used for WFIRST. However, this approach also necessitates the generation of an intermediate simplified analysis CAD model in order to apply meshing rules and generate the thermal and structural finite element models. This intermediate, simplified geometry was a significantly new way of developing CAD models as it required the abstraction of a three-dimensional solid model to two-dimensional surfaces where appropriate to be able to be meshed. This step is often locally performed by the thermal or structural analysts in their analysis tools and under the discretion and control of the analyst. This effort was now shifted to the mechanical engineer in the solid CAD package. As such, it required significant time and effort to generate the "analysis CAD" for the new tool. The drawback to this was that the efforts to push the design forward suffered since the primary mechanical designers' efforts were focused on building the analysis CAD rather than evolving the details of the current design.

Lesson Learned: Efforts to evaluate new tools within the course of normal design work should be performed in parallel by additional personnel if possible to minimize the impact on design evolution.

V. CYCLE 4 DESIGN

During the Cycle 4 design, some details began to clarify for the use of the existing AMS hardware regarding allowable load limits and lines of action. The latch locations of the WFI changed, with the A-Latch moving closer to the other two WFI latches to make the plane between the latches parallel to the AMS. The truss tube structure of the Cycle 3 Instrument Carrier (Figure 4) was no longer needed as both instruments latched to the sandwich composite Instrument Carrier structure. Another major science requirement change (FPA detector temperature from 120 K to 100 K necessitated the introduction of a cryocooler with a pumped neon loop to cool the detectors and the cold electronics together as one package. A cryo heatpipe was envisioned to transport the heat from the detector assembly to the cryocooler heat exchanger. Consequently, the radiator for cooling the FPA was now rejecting heat at a much

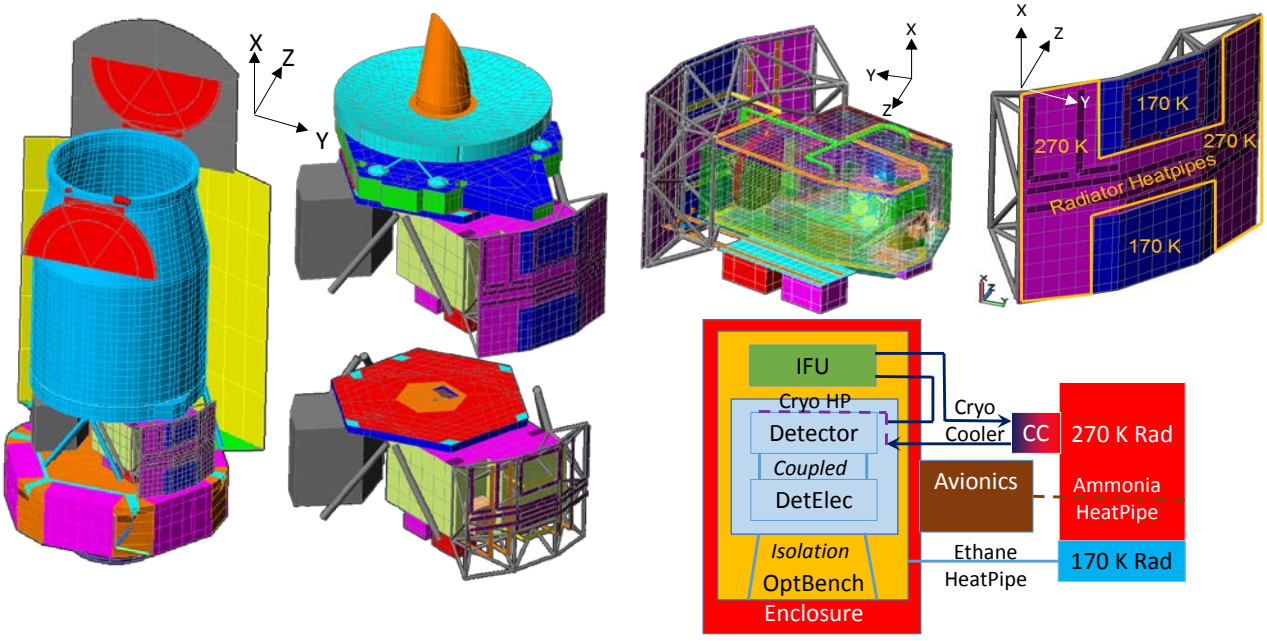

Figure 4. WFIRST Observatory Cycle 4 Thermal Model: *Telescope, AMS, Instrument Carrier no longer includes truss; WFI with 270 K and 170K radiators and instrument side avionics, and CGI (Top Right), and Instrument Carrier, CGI and WFI Enclosure and Heatpipes (Bottom Right).*

Figure 5. WFI Instrument Cycle 4 Thermal Model: *optical bench cooled by top and bottom ethane heatpipes connected to 170 K radiators, instrument avionics coupled to H-shaped 270 K radiator via ammonia heatpipes; Cryocooler compressor mounted to 270 K radiator.*

warmer temperature due to the cryocooler. Cycle 4 also addressed a major perceived lien against the Cycle 3 design regarding the serviceability of the WFI instrument; the Cycle 3 design required serviceable connections for over 1000 wires based on the science signals from the WFI FPA. To address this, the warm instrument electronics (Focal Plane Electronics and Command and Data Handling) boxes were moved from a spacecraft bay to locations on the instrument to allow for a more modular approach to serviceability (Figure 5). These instrument side warm avionics were thermally coupled via ammonia heatpipes to the same radiator for rejecting the cryocooler dissipation. The cooling of the optical bench was still achieved passively with ethane pipes, but a top and bottom radiator were introduced and replaced the picture frame radiator from Cycle 3 to reduce the vertical gradient in the optical bench. A consequence of the Cycle 4 design was a heavier and larger overall instrument with the structure now needing to be strong enough to support the additional instrument side avionics boxes. This growth exacerbated a major lien against Cycle 4 since the existing AMS hardware was found to have significant limits on its mass support capability.

VI. CYCLE 4 LESSONS LEARNED

During the processing of results from early Cycle 4 model runs, the view from the primary mirror to the inside of the outer barrel assembly was considerably lower than expected. Investigation into the nodal radiation couplings between the primary mirror and the outer barrel assembly revealed that a number of expected views were missing from the output. Further study of the missing radiation couplings revealed an interesting feature of the radiation coupling filtering for nodes assigned to multiple surfaces and combinations of high and low emissivity. Figure 6 shows a section of a facesheet-core-facesheet mirror construction, with the highly reflective (low emissivity) surface on the top and typically high emissivity surface on the back of the front facesheet and the internal ribbing. In the Cycle 4 model, the internal faces of the primary mirror were erroneously included in both the external radiation enclosure as well as the internal primary mirror enclosure, while they should have been included only in the internal radiation enclosure. Nonetheless, including these surfaces in the external group in theory should produce no error. However, the radiation coupling filtering applied to reduce the total number of small terms passed to the thermal solver did end up eliminating these terms. For any given node on the front of the mirror, the overall ratio of emissive capability for the reflective vs. non-reflective surfaces is on the order of 127:1 (0.85*12 : 0.02*4) Therefore, when including the top 95% of B_{ij} contributors, the high emissivity internal surfaces are a significantly higher contributor to the overall emissive capability than the low emissivity (high reflectivity) external surface contributions. Since the software is indiscriminant as to what level of filtering should be applied locally and applies a global approach, these contributions are neglected. The solution in this case was to remove the internal surfaces from the external radiation calculations, which leaves only the low emissivity surfaces to contribute and 95% of the low emissivity terms are included in the final outputs. This approach is acceptable for a closed back mirror, but may not suffice for an open back design. Radiation analyzer software developers should consider the addition of selective identification of critical surfaces for which different or no filtering rules should be applied to minimize the impact of this effect.

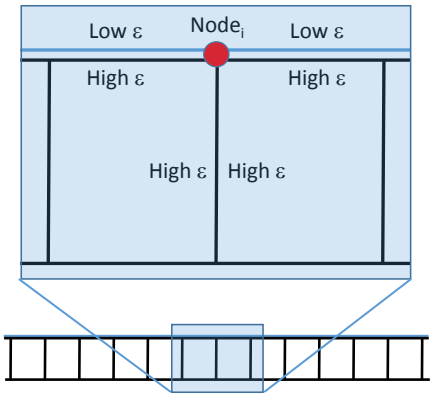

Figure 6. Primary Mirror Segment: *For Node i, $\Sigma B_{ij} \approx$ Front Surface Top + Front Surface Bottom + Both faces of Ribs $\approx$ (4*A*Low ε) +(4*A*High ε)+ (8*A*High ε). Front surface accounts for only about 0.8% of emissive capability, which may get filtered.*

Lesson Learned: Couplings for the reflective side of critical optical surfaces with both sides active and significantly different optical properties on each side may be eliminated by radiation coupling filtering.

The FPA design was also updated from Cycle 3 to account for a cryocooler. The Cycle 3 design featured a large temperature difference between the passively cooled detectors at 120 K and the passively cooled cold electronics at 170 K. This temperature difference was maintained by a low conductivity composite frame supporting the two components that was also isolated via a set of three bipods from the optical bench. For Cycle 4, with the introduction of a cryocooler, the design included a single heat exchanger for the entire FPA assembly that cooled both the detectors and the cold electronics. The frame was changed to a high conductivity composite to minimize the temperature differences between the detectors and electronics. The set of three bipods still maintained their thermally isolative design. Lastly, a pair of nitrogen or oxygen heatpipes attached to the detector mounting plate transported the heat to the single cryocooler heat exchanger for the FPA.

Modeling the cryocooler itself was also a challenge. The cryocooler is baselined as a reverse Brayton cycle, turbomachine that circulates cold neon gas through a cooling loop. This cryocooler meets the low vibration requirements necessary for precise observatory pointing. Performance curves for the cryocooler were obtained for various input loads, cooling setpoints, and hot side rejection temperatures. A neon fluid loop was included in the model using the FloCAD® module within ThermalDesktop® to define a pipe, but only simulated the cooling loop and not the fluid mechanics of the cryocooler itself. This pipe was assigned the necessary properties and connections to include two heat exchangers (one at the IFU and one at the FPA) and simulated the cooling loop from the supply exit of the compressor back to the return inlet to the compressor. The total load into the cooling loop was calculated at each timestep and passed to the lookup logic along with the radiator temperature and desired setpoint. The performance curves were used to compute the necessary mass flow rate, compressor power, and electronics power for a given input set of loads, achieved temperatures and desired setpoints. This mass flow rate was then assigned to the SetFlow object in FloCAD®.

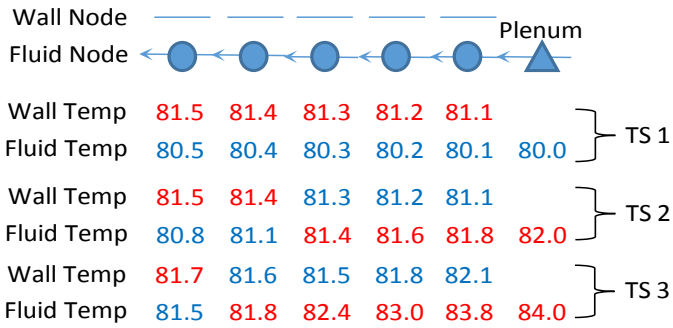

Figure 7. Transient behavior of Line Inlet: *Setting inlet temperature transiently can result in heating instead of cooling at inlet if not properly modeling a closed fluid loop*

This quasi-steady control approach assumes the controller will achieve the setpoint with no error and was initially developed to set the inlet temperature and mass flow rate. The inlet temperature necessary to achieve the desired setpoint was estimated from the setpoint minus the total load removed divided by the projected mass flow rate and specific heat ($T_{inlet} = T_{setpoint} - Q/(\dot{m} \times C_p)$). This computed inlet temperature was initially set as the plenum temperature (a fluid boundary node) along with the mass flow rate. However, this approach did not work well in practice. The physical behavior of the loop should be a steady increase in temperature from the cryocooler supply line through the system with the hottest temperature at the return line to the cryocooler. Correspondingly, the tube wall temperatures should also be above the corresponding fluid node temperature due to the cryocooler supplying the cold gas. Analytically, however, the changing of both the mass flow rate and loop inlet temperature did not produce this behavior. If the plenum temperature is increased as a result of this computation, the higher inlet temperature may actually provide some heating of the tube close to the cryocooler (Figure 7) and begin to cool down until an adiabatic condition is met further downstream. At this point, the initial heating provided by the fluid would have been transferred to the wall and the remaining fluid in the loop begins to warm up due to the warmer surroundings. A further constraint would have been necessary to ensure that additional heat is not added to the system in terms of an inlet temperature that was higher than the inlet wall node. To proceed with the analysis and meet the schedule for simulation results, the plenum temperature was fixed at a boundary and only the mass flow rate was updated; the exact cause of the erroneous behavior was not further investigated to fully understand the root cause. Without a closed loop simulation of the entire fluid behavior throughout the cryocooler, this was judged the best approach based on available data and models. Future versions of the model will include the fluid behavior of the entire cryocooler and PID controller as provided by the cryocooler vendor and not just the cooling loop. This will be critical to predict the stability of the control system, which is currently not as accurate as desired with a fixed inlet temperature.

Lesson Learned: In order to predict correct results, it is important to ensure that models account for proper physics and that the analyst fully understands the expected behavior. Furthermore, understanding deficiencies in the model can also help to identify further information needed to improve the predictions.

VII. CYCLE 5 DESIGN

The Cycle 5 design addressed the major lien from Cycle 4 that the existing AMS hardware was unable to support the mass of the Instrument Carrier, CGI, and WFI instruments. To solve this, the Instrument Carrier's role was increased from simply supporting the two instruments to now supporting the telescope itself as well as the two instruments. The Cycle 5 design features a composite truss like structure that surrounds the two instruments and supports the AMS and accompanying telescope via shorter bipods. Longer, vibration isolating bipods to the spacecraft deck now supported the Instrument Carrier. The solar arrays now deploy to a single flat plane rather than remaining angled and fixed as in the previous designs. The FPA design was also modified from Cycle 4 to add an

additional heat exchanger for the cold electronics and the flow direction reversed to cool the IFU, FPA Detectors and the FPA Cold electronics in that order (Figure 8). This eliminated the need for the nitrogen or oxygen heatpipes in the FPA, which were a low technology readiness level component. With the separation of detectors and cold electronics thermally, the frame was changed back to a low conductivity composite as in Cycle 3, since the temperature of the cold electronics was not as much a driving requirement as the temperature of the detectors.

The move of the instrument electronics boxes was also revisited for Cycle 5. Assumptions made about the difficulty for servicing to accommodate the harness connections between the electronics and optics module were further investigated. With the overall increase in mass and complexity to accommodate the electronics on the instrument side, the decision was made to relocate the electronics boxes back to the spacecraft bays with the assumption of a more dexterous servicing capability than believed during Cycle 3.

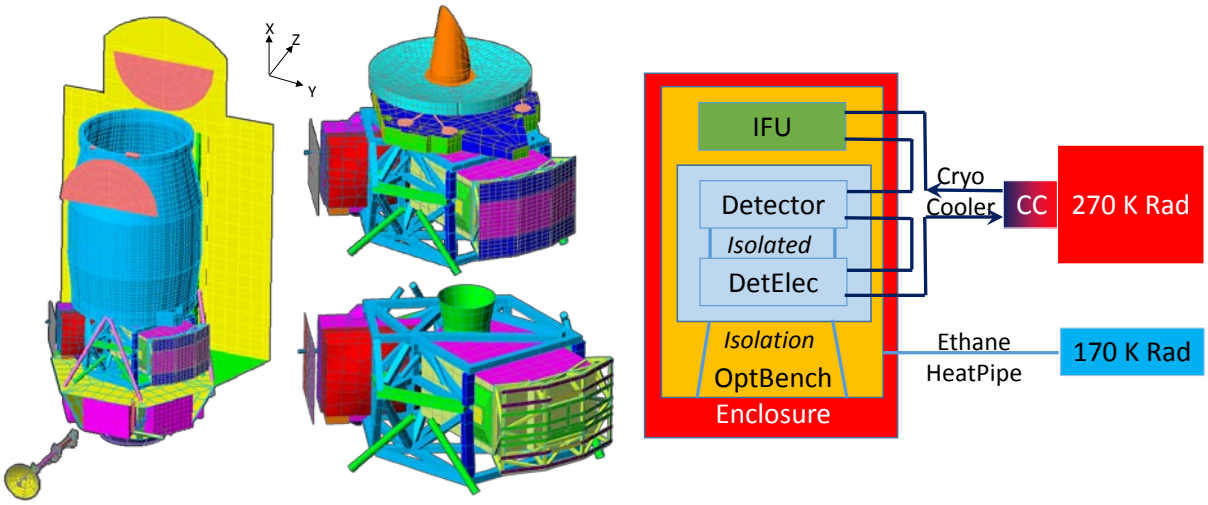

Figure 8. WFIRST Observatory Cycle 5 Thermal Model: *Telescope, AMS now supported by Instrument carrier, Instrument Carrier now a truss structure with no sandwich plate on top, WFI with 270 K and 170K radiators and no instrument side avionics, and CGI (Top Middle), and Instrument Carrier, CGI and WFI Enclosure and Heatpipes (Bottom Middle) and WFI Thermal Block Diagram (Right)*

VIII. CYCLE 5 LESSONS LEARNED

During the Cycle 4 design process, it became increasingly apparent that designing the Instrument Carrier, CGI, and WFI to be supported by the AMS would be very challenging due to the AMS having been designed and built to support a different payload than the WFIRST instrument suite. Furthermore, the limited availability of information regarding its exact capabilities and the relatively rapid wind down of the original program further made designing the WFIRST hardware very difficult. A number of trade studies were launched during Cycle 5 to find a way to preserve the baseline approach of supporting the instruments from the AMS, including: moving optics from the instrument to the Instrument Carrier, separation of optics and electronics into different modules but still locating them in the Instrument Carrier, use of additional inserts in AMS turtle tail or relocation of instruments to better take advantage of the existing AMS, support of instruments from spacecraft rather than the AMS, and redesigning the Instrument Carrier to support the AMS and instruments rather than the current design of supporting the carrier and instruments from the AMS.

The first option of moving the first fold mirror and the first powered mirror to be supported as relay optics by the Instrument Carrier was deemed to be too difficult to implement, align, and test at instrument level and was relatively quickly eliminated. The option to separate the instrument electronics and optics/detectors into separate modules, but leave them connected by a non-serviceable harness was fully investigated. This option was desirable to minimize the load supported by the AMS for the optics module, while providing for the near co-location of the electronics module supported by the spacecraft below the optics module (the so-called 2 drawer design). This option maintained that the instrument modules would be installed or removed as a unit with the high wire count harness between them not being disconnected. This option was discarded due to a necessary growth in the overall height to accommodate the design as well as risks associated with latching and delatching the two portions together for servicing.

Other options investigated the possibility of utilizing additional inserts in the AMS turtle tail to support the CGI instrument entirely or a portion of the WFI instrument. These options were also relatively quickly eliminated as being non-viable due to the impact on the overall optical design relative to the telescope as well as the limitation on the lines of actions for the inserts in the AMS and load limitations of the fittings. Another option that was investigated was the possibility of two sets of latches for the WFI. During launch, the WFI instrument would be supported by the spacecraft. Once in flight, the latches would release and a mechanism would raise the instrument up to latch into the AMS. Since the limitations of the fittings are due to loading during launch, the support of the AMS in a zero gravity environment does not have the same limits and constraints. The largest concern with this approach was the ability to ensure proper alignment between the telescope and the instruments post-deployment in flight, which would be challenging to verify in the presence of gravity during ground testing.

The last option, and the one pursued for Cycle 5, was to remove the AMS from the support load path for the Instrument Carrier, CGI, and WFI. A new Instrument Carrier was designed that was supported with D-Strut bipods from the spacecraft deck. This new Instrument Carrier design supported the WFI, CGI, and now the AMS and telescope. This solution no longer utilizes the inserts of the AMS to support the instrument payload and consequently eliminates the concerns for overloading the existing hardware. However, it does introduce a new concern regarding the optical metering between the telescope and the instruments.

Lesson Learned: While use of existing hardware has the appeal of apparent lower cost and schedule impacts, the efforts to accommodate potential limitations of hardware not designed for a specific mission's needs may result in increased cost, schedule, and complexity elsewhere in the program.

One requirement that has consistently driven aspects of the design without being well-defined is serviceability. A lack of concrete definition has been a design driver in more than one occasion. The need for all the spacecraft avionics bays to be serviceable greatly limits the available locations to mount boxes. The location of three of the bays on the sun side provides a much less than optimal sink temperature for radiators, further limiting the arrangement of boxes based on power. With this serviceable bay arrangement, a single large radiator with multiple avionics cannot be utilized to share in the power growth risk, and each bay carries the risk that its particular components' power growth may later exceed its radiative capabilities. Furthermore, the harness aspect between the bays cannot be optimized due to the inflexible constraints of heat rejection and mechanical packaging; a very limited number of configurations of avionics resulted in viable designs from a packaging and thermal point of view.

The serviceability of the instruments has also driven the design with considerations for the removal and replacement of the WFI and CGI. In particular, the WFI requires over 1000 wire connections between the detector cold and warm electronics without the addition of a multiplexer. Over the last year this has very much driven the design to first move the instrument electronics boxes to the instrument side to mitigate this risk, but the consequence in the associated mass growth was deemed unacceptable at this phase and the boxes were moved back to the spacecraft side. Additionally, the capabilities of servicing remain unclear at best, with concrete definitions of robotic servicing capabilities lacking. Most recently, the power needs during servicing, particularly for heating the outer barrel assembly have caused concerns with the ability of the servicing to address WFIRST's needs. Designing to possible future capabilities carries a mass and complexity penalty that is difficult at best to quantify.

Lesson Learned: Designing for serviceability should be very clearly defined from the outset, considering many factors such as scope of serviceable components, existing redundancy and reliability, demand from science community for future upgrades, and additional complexity introduced by being serviceable.

IX. CYCLE 6 AND BEYOND

The Cycle 6 design will study to feasibility of a mission orbiting the second Earth/Sun Lagrange point (L2) instead of a geosynchronous orbit. This consequently results in a much more stable environment without the Earth thermal disturbance and Earth/moon field of regard constraints. The Cycle 5 design is currently in the closeout process and the project is evaluating the liens on the Cycle 5 design in preparation for more formal trade studies as part of Cycle 6. A trade study is underway to mechanically and thermally separate the detectors from the cold electronics and cool only the detectors via the cryocooler, allowing the cold electronics to run warmer. An additional heat path will be provided for the cold electronics to remove their heat. This trade will optimize the radiator size and consequently the associated mass. Another follow-on trade study planned is to evaluate the possibility of passively cooling the FPA rather than actively cooling with the cryocooler. These trade studies among others kick off at the beginning of the Cycle 6 design phase leading to an Internal Concept Review in late 2015. One additional design cycle is envisioned before a Mission Concept Review is held in June 2016, leading to entry into Phase A in October 2016.

X. CONCLUSION

The designs from Cycle 3 through Cycle 5 have explored the trade and design space, seeking the optimal performance, cost, mass, power and volume for the mission and instruments. Even before Phase A, the WFIRST design and analytical models have grown in maturity to address challenging stability and performance requirements along with the challenges of accommodating existing hardware and designing around the uncertainty of serviceability. The models have tested and vetted the analytical process for detailed design modeling and STOP analysis to characterize the performance of the entire system. While the model complexity has grown, the predicted results have been consistent with expected physical behavior.

The Cycle 5 effort is concluding and the Cycle 6 design effort is to begin soon. The risks inherent to the donated telescope hardware are being mitigated to fully take advantage of this cost reduction opportunity by the WFIRST mission, which greatly reduces the overall mission cost. As the design has evolved, the funding levels have also increased with significant risk reduction efforts already underway. These include the design and build of the Element Wheel and F2 mirror assemblies, detector characterization, and grism testing. Further risk reduction efforts are currently beginning including an ambient optical bench testbed to ensure the system can be optically aligned. WFIRST is poised to enter formulation in October 2016 and in the future provide an observatory with unprecedented capabilities to image the infrared sky, search for Exoplanets, and answer key questions about Dark Energy and its role in the accelerating expansion of the Universe.

Acknowledgments

The authors would like to thank the entire team for their tireless efforts to design, analyze, and push massive amounts of data and analysis through to complete numerous STOP cycles. These analysis included numerous points over long slew periods simulating the worst case or most representative for the CGI and WFI instruments. The responsiveness and collaboration of the entire team to rise up to the schedule challenges, both planned and unexpected, has been remarkable.

Lessons Learned Summary

Lesson Learned: For tight temperature control, the inclination to set a small control band may lead to poor performance of a proportional controller. A larger temperature control band will likely improve the stability.

Lesson Learned: Efforts to evaluate new tools within the course of normal design work should be performed in parallel by additional personnel if possible to minimize the impact on design evolution.

Lesson Learned: Couplings for the reflective side of critical optical surfaces with both sides active and significantly different optical properties on each side may be eliminated by radiation coupling filtering.

Lesson Learned: In order to predict correct results, it is important to ensure that models account for proper physics and that the analyst fully understands the expected behavior. Furthermore, understanding deficiencies in the model can also help to identify further information needed to improve the predictions.

Lesson Learned: While use of existing hardware has the appeal of apparent lower cost and schedule impacts, the efforts to accommodate potential limitations of hardware not designed for a specific mission's needs may result in increased cost, schedule, and complexity elsewhere in the program.

Lesson Learned: Designing for serviceability should be very clearly defined from the outset, considering many factors such as scope of serviceable components, existing redundancy and reliability, demand from science community for future upgrades, and additional complexity introduced by being serviceable.